Haptic Exploration for 3D Shape Reconstruction using Five-Finger Hands

A. Bierbaum, K. Welke, D. Burger, T. Asfour, and R. Dillmann
University of Karlsruhe
Institute for Computer Science and Engineering (CSE/IAIM)
Haid-und-Neu-Str. 7, 76131 Karlsruhe, Germany
Email: {bierbaum,welke,asfour,dillmann}@ira.uka.de

***Abstract*—In order for humanoid robots to enter human-centered environments, it is indispensable to equip them with the ability to recognize and classify objects in such an environment. A promising way to acquire the object models necessary for object manipulation appears in the supplement of the information gathered by computer vision techniques with data from haptic exploration. In this paper we present a framework for haptic exploration which is intended for use with both, a five-finger humanoid robot hand as well as with a human hand. We describe experiments and results on haptic exploration and shape estimation of 2D and 3D objects by the human hand. Volumetric shape data is acquired by a human operator hand using a data glove. The exploring human hand is located by a stereo camera system, whereas the finger configuration is calculated from the glove data.**

I. Introduction

In humans, different types of haptic exploratory procedures (EPs) for perceiving texture, weight, rigidity, contact, size and the exact shape of a touched object are known [1]. These EPs require the exploring agent to initiate contact with the object and are therefore also referred to as active touch sensing.

In this paper, the contour following EP for shape recovery is subject of interest. A volumetric object model composed this way delivers a rather high amount of information for discriminating between objects. Also, volumetric object data is most suitable for supplementing and verifying geometric information in multimodal object representations.

Several approaches have been proposed for acquiring object shape information by robots through haptic exploration. An early, comprising experimental setup was presented in [2], where a dextrous robot hand was used in conjunction with a manipulator arm. The hand probed contact by enclosing the test objects at predefined positions and evaluating joint angle and force readings. The resulting sparse point clouds were fitted to superquadric models defined by a set of parameters describing shape and pose.

In addition to the contact locations, the contact normal information gathered during haptic exploration was used in [3]. Instead of a superquadric model here a polyhedral model was chosen as volumetric object representation. For object recognition the Euclidian distances of the polyhedral surface points to the borders of a surrounding cubic workspace box were measured at equidistant intervals and matched to those of synthetic models. This approach was evaluated only in simulation.

The basic kinematics of contact and its application in contour following are presented thoroughly in [4]. Moreover, several procedures for haptic exploration of object features have been investigated in [5], [6]. Other approaches in active contact sensing concentrate on the detection of local surface features [7].

In our approach, a framework has been developed that allows haptic exploration of unknown objects for recovery of the exact global shape using different types of manipulators equipped with contact sensing devices. This separates our work from approaches involving model based pose estimation of known objects as in [8].

As we are interested to integrate the framework as basis for haptic exploration in our humanoid robot system [9] which is equipped with two five-finger human-like and human-sized hands, we focus on the application of exploring with five-finger hands. In particular, the developed framework allows us to use the human hand of an operator as exploring manipulator by deploying a data glove with attached tactile sensors. This gives us the opportunity to already investigate the EPs of interest until the humanoid robot hand is fully integrated into our robot. It also provides rich possibilities for immediate comparison of haptic exploration results by a human versus a humanoid robot hand.

Our aim is to establish a robust exploratory process for 3D shape reconstruction and modeling which can be performed in an unstructured environment, while only providing observability of the hand pose, the finger configuration and the contact information. Currently we are limited by the constraint that the object being explored must remain in a fixed pose.

As modeling primitive we chose an extended superquadric function as in [2] which can represent a variety of cubical and spherical geometries. In the context of grasp planning this type of representation has just recently been investigated for modeling physical objects by superquadric decomposition [10]. Yet, in this paper we only address modeling of basic superquadric shapes. Also, we can not give results related to non-convex objects at this stage of our work, as those are not reflected by the chosen model, although the exploration process itself is not limited to convex objects.

This paper is organized as follows. In the next section the relevant details and components of our system for haptic exploration focusing on object shape recovery are described. This includes a description of the human hand model and visual tracking of the operator's hand. In Section III we present experiments on haptic exploration of 2D and 3D real world objects. Finally we give a conclusion and an outlook on our future work in SectionIV.

II. System description

Figure 1 gives a system overview with the components involved in acquisition of contact points during contour following EP.

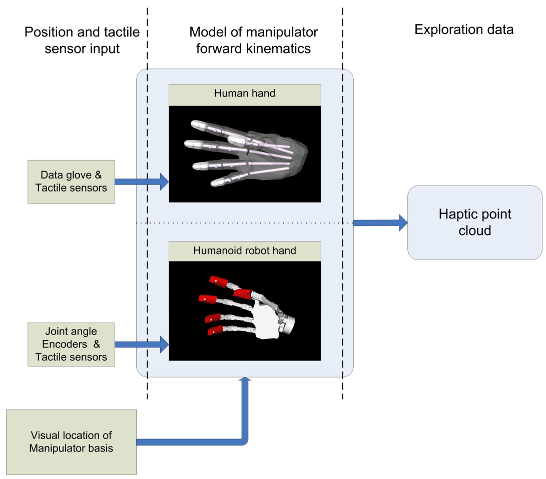

Fig. 1. System for acquisition of object shape data from haptic exploration using a human or a humanoid robot hand as exploring manipulator.

During haptic exploration with the human hand, the subject wears a data glove that serves as an input device for calculating the joint angle configuration of the hand. The data glove we use is equipped with binary micro switches at the distal phalanges. When touching an object, the switches are actuated as local contact force exceeds a given threshold. During actuation the clicking of the switch also provides the operator with a mechanical sensation, that helps to control the contact pressure during exploration. The data glove is made of stretch fabric and uses 23 resistive bend sensors that provide measurement data of all finger joint angle positions and the orientation of the palm.

Before starting exploration the operator needs to calibrate the data glove sensors with the forward kinematics of the underlying hand model. Subject to calibration are abduction/adduction and flexion/extension of all fingers, curvature of the palm and the thumb motion.

A linear relation is used for projecting glove sensor readings to joint angles. Calibration is accomplished by engaging positions which result in minimum and maximum sensor response in a separate calibration procedure.

Wrist position and orientation are determined visually in the reference frame of the camera coordinate system as described in Section II-B. During exploration the subject visually guides the finger tips following desired paths. When the micro switch is actuated by touch, the current location of the sensor in the global reference frame is registered as a point in the 3D object point cloud. The sensor position is calculated using the forward kinematics of the hand model as described in the following section.

For exploration with our humanoid robot platform ARMAR-III we may later use a model for the forward kinematics of the robot hand as presented in [11]. The robot is equipped with an advanced version of this hand with joint angle encoders attached to all controllable degrees of freedom (DoF) and tactile sensors at the fingertips.

The data acquired as 3D point coordinates in the haptic point cloud set is finally used for performing a superquadric model estimation.

A. Human hand model

The forward kinematics of the human hand must be modeled accurately to transform the coordinates of the tactile sensor locations gathered from the data glove sensor readings to a global reference frame in which the resulting 3D contact point cloud is accumulated. Furthermore, the model is required to cover the entire common configuration space of the human hand and the data glove, so that the human operator is preferably not restricted in the choice of hand movements that can be projected to the model.

A complex hand model deploying 27 DoFs was introduced in [12] and used in several studies requiring exact models ([13], [14]) for hand pose estimation from sensor input. The Carpometacarpals joints (CMC) were fixed, assuming the palm to be a rigid part of the hand. The fingers were modeled as serial kinematic chains, attached to the palm at the metacarpophalangeal joints (MCPs). Interphalangeal joint (IP), distal interphalangeal joints (DIP) and proximal interphalangeal joints (PIP) have one DoF for flexion and extension. All MCPs joints have two DoFs, one for flexion and extension and one for abduction and adduction. The CMC joint of the thumb is modeled as a saddle joint. Several variants of this model exist in literature (see [15], [16]).

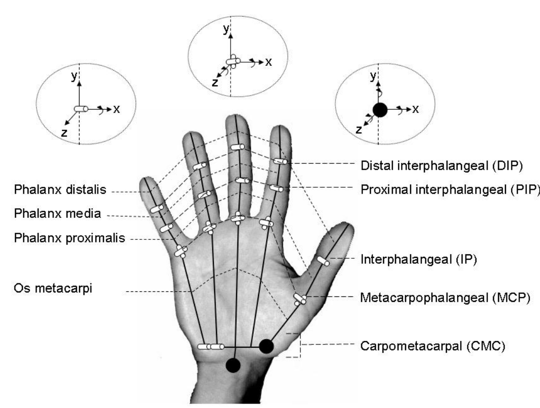

Fig. 2. The used hand model for haptic exploration by a human operator wearing a data glove.

The hand model we use in the presented framework is shown in Fig. 2. We have added two modifications to the basic model to improve the representation of real human hand kinematics. The first modification affects the modeling of the thumb's CMC joint. Following [16], the first metacarpal of the thumb performs a constrained rotation around a third orthogonal axis in the CMC joint, which contrasts the CMCs joint model as a two DoF saddle joint. For reasons of simplicity we model this joint as a three DoF joint.

The second modification is to overcome the inadequate representation of the palm as a rigid body. As we want to incorporate the distal phalanges of the ring and little finger in the exploration process, we have extended the model by adding one DoF at the CMCs of these fingers respectively. By doing this the ability of the palm is reflected to fold and curve, when the little finger is moved towards the thumb across the palms inner side [17]. It is important to model this behavior as a human operator will occasionally utilize these types of movement when touching an object with the whole hand.

The resulting hand model consists of 26 DoFs. The four fingers have 4 DoFs each at the DIP, 4 DoFs at the PIP and 8 DoFs at the MCPs. The thumb is modeled with 1 DOF at its IP, its MCP is modeled with 2 DoFs and its CMC, as mentioned before, with a 3 DoF joint. Additionally we model the palm with 2 DoFs representing the CMCs of the little and ring fingers and add 2 DoFs for the wrist movement.

We have used the Open Inventor™ [1] standard for constructing the hand model. This 3D modeling package allows the implementation of local reference frames as described before in a transparent way.

B. Wrist tracking

As mentioned earlier, the absolute position and the orientation of the data glove are determined using vision. In order to track the data glove in a robust manner, we use a marker bracelet which is attached to the wrist of the subject wearing the data glove and is tracked using a stereo camera system. Figure 3 shows the marker bracelet used for our experiments. The bracelet comprises twelve red markers for tracking and one green marker for initialization. All markers are printed on yellow background. The wrist localization consists of two phases. In the initialization phase, the pose of the wrist is estimated without the knowledge of past poses. Once an initial pose has been calculated, a particle filter approach is used to track the pose of the wrist.

For the initialization, the relevant markers are identified by HSV color segmentation performed in the current scene. Only green and red markers inside yellow areas are considered for color segmentation. With the calibration of the stereo camera system, the 3D coordinates of the green marker and the second and third closest red markers are calculated. Since these markers lie all in the same plane, the plane normal can be calculated from this information. Given the radius of the bracelet, the center of the circle described by the three

[1] http://oss.sgi.com/projects/inventor/

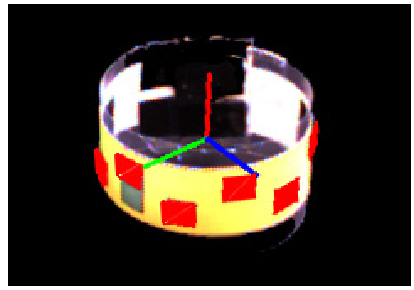

Fig. 3. Bracelet and coordinate system.

considered markers may be calculated. The x-axis of the coordinate system (denoted red) can be derived from plane normal and center. The y-axis (denoted green) is calculated from the difference of the green marker and the center. The z-axis is calculated as the cross product of x- and y-axis.

After initialization, the bracelet is tracked using a particle filter [18] based on a model of the bracelet comprising all 12 red markers. The configuration of the model is defined by the 6D pose of the band. In each iteration of the particle filter algorithm 100 new configurations are generated using a gaussian distribution with variance $\sigma^2 = 0.45$. Furthermore the movement of the model is estimated by taking into account the movement in the previous frame. In order to retrieve the estimated 6D pose of the wrist band, the visible part of the model is projected into both camera images using the camera calibration. To validate each particle, a weighting function is used which compares the segmentation mask for the red color with the model. In order to derive a weighting function for each configuration, we count all red pixels inside yellow regions f and all red pixels, which overlap with the projected model m. The probability for each particle z and the current images i can then be formulated in the following way:

$$p(z|i) \propto exp\left(\lambda * \frac{m}{f}\right)$$

where λ defines the sector of the exponential function which is used. After all particles have been weighted according to this equation the 6D pose is estimated by the weighted sum of all configurations.

C. Superquadric fitting for shape estimation

The concept of superquadrics has been introduced in [19] as a family of parametric 3D shapes, among which the superellipsoid has become the most popular one and therefore is often termed as superquadric, a convention we will preserve here.

A superquadric centered in the origin and with its axes aligned to the x, y, z coordinate axes can be described with the following parametric equation

$$\chi(\eta, \omega) = \begin{pmatrix} a_1 \cos^{\varepsilon_1}(\eta) \cos^{\varepsilon_2}(\omega) \\ a_2 \cos^{\varepsilon_1}(\eta) \sin^{\varepsilon_2}(\omega) \\ a_3 \sin^{\varepsilon_1}(\eta) \end{pmatrix} \quad .$$

The parameters a_1, a_2, a_3 describe the extent of the superquadric along each axis. The exponents ε_1, ε_2 ϵ $[0..2]$ produce a variety of convex shapes and describe the shaping characteristics from cubic to round in x and y directions. This way different 3D primitive shapes can be modeled, e.g. boxes $(\varepsilon_1, \varepsilon_2 \approx 0)$, cylinders $(\varepsilon_1 = 1, \varepsilon_2 \approx 0)$ and ellipsoids $(\varepsilon_2 = 1)$.

To locate the superquadric arbitrarily in space, we further introduce a rotational matrix $\mathbf{R}$ and a translation vector $\mathbf{x_0}$, which add 6 more parameters to our model.

As superellipsoids are restricted to symmetric shapes only, we also add deformation parameters $\{t_x, t_y \ \epsilon \ [-1..1]\}$ for modeling tapering in z direction as described in [20]. This enables our model to also represent wedge resembling shapes. Applying a scaled tapering deformation function

$$D_t(x, y, z) = \begin{pmatrix} t_x \frac{z}{a_3} + 1 \\ t_y \frac{z}{a_3} + 1 \\ 1 \end{pmatrix} \begin{pmatrix} x \\ y \\ z \end{pmatrix}$$

we finally get the model function

$$\mathbf{m} = \mathbf{R} D_t(\chi(\eta, \omega)) + \mathbf{x_0} \quad .$$

To estimate the 11 parameters of our superquadric model from the 3D contact point data we use the Levenberg-Marquardt non-linear least-squares algorithm [21] to minimize the radial Eucledian distance d between the data points and the superquadric surface

$$d = \|\mathbf{x}\| \left(1 - \frac{1}{F(\mathbf{x})}\right) \quad .$$

as proposed in [22]. Here, $F(\mathbf{x})$ is the inside-outside function of the superquadric, which has a value of 1 for points $\mathbf{x} = (x, y, z)^\top$ on the surface of the superquadric, while points inside result in $F < 1$ and points outside result in $F > 1$.

III. Experiments for Object Shape Recovery

For evaluation of the system described above we have performed experiments related to the exploration by a human subject. The experimental setup hereby is shown in Fig. 4.

The region viewable by the stereo camera system defines the workspace in which the objects to be explored have to reside. The human operator wears a data glove with the wrist marker attached and performs a contour following EP with the tip of the index finger upon the object, i.e. the human operator visually guides the contact sensor along the contours. As mentioned earlier, the micro switch for contact sensing is also located at the distal phalanx. During the EP the object is fixed within the workspace. The human operator is allowed to move hand and fingers arbitrarily within the workspace as long as the marker bracelet may be visually detected and localized. In case the marker localization fails, the subject needs to move the hand until it can be detected again.

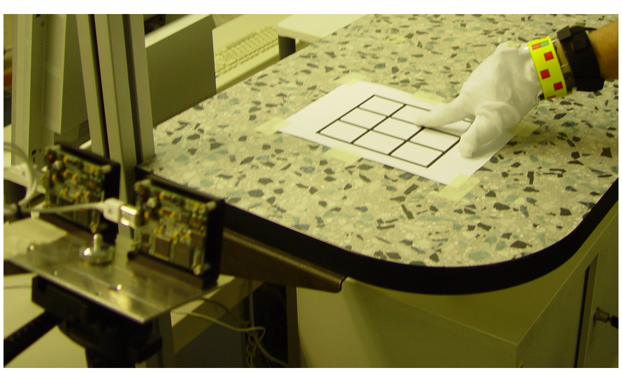

Fig. 4. Experimental setup. Here a planar grid structure is subject to contour following.

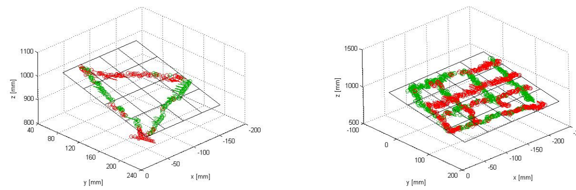

(a) Triangle contour (b) Grid structure contour

Fig. 5. Resulting point clouds for tactile contour following of planar shapes and corresponding fitted planes. Red points are situated below the plane, green points above.

A. 2D contour following in 3D space

As an initial experiment we chose to follow the visible contours of a planar structure to verify whether the exploration system delivers length and angle preserving point clouds. These properties were inspected visually from the resulting point cloud data. We calculated the PCA for all points in the point cloud for approximation of the plane the structures are located in. Further, we determined the standard deviation of the point locations in respect to this plane.

As planar shapes we chose a circle, an isoceles triangle and a 3×3 grid. The edge length of the bounding box for each of these shapes was set to $160mm$. The subject followed the contours of a printout of the respective shape with the index finger. Resulting point clouds for triangle and grid contours are shown in Fig. 5. The figures show that the contours of the test shapes are situated in different planes, which originates from a change in the position of the camera system between the two explorations. The duration of the exploration process was 40 seconds for the circle and triangle shapes and 2 minutes for the grid structure. Exploration speed was mainly limited by the performance of the wrist tracking algorithm.

During circle contour following 245 contact points were acquired, the standard deviation to the fitted plane was calculated to $\sigma = 5.37mm$. For the triangle contour following exploration 259 data points were acquired with $\sigma = 6.02mm$. For the grid exploration finally, 1387 data points were acquired with $\sigma = 5.86mm$.

B. Edge tracking of a 3D object

In this experiment the subject had to follow the edges of a rectangular box situated on a table in the workspace. The exploration procedure delivered 1334 data points, the resulting

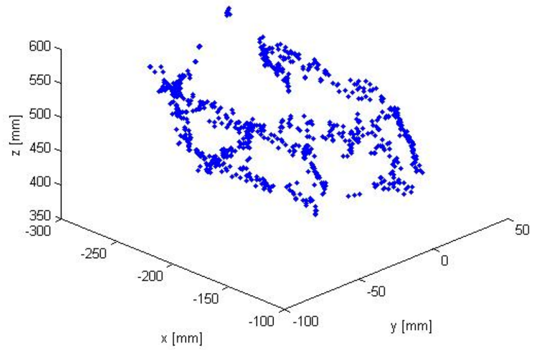

Fig. 6. Resulting point cloud for haptic contour following of a rectangular box.

point cloud is depicted in Fig. 6. The box dimensions were $150 \times 50 \times 120mm$ and therefore in the range of the dimension of the human hand itself.

It is not possible to directly fit exploration data to a superellipsoid which comprises only points from the edges of an object as the data is ambiguous in describing the adjacent surfaces without having additional surface normal information. Yet, we wanted to proof the systems capability to generate contiguous 3D point clouds of real world objects.

C. Arbitrary touch exploration and superquadric fitting of a 3D object

In a further experiment the exploring subject acquired contact coordinate information by arbitrarily touching all reachable surfaces of the objects while no preference was given to the edges. For exploration a different box and an upside-down placed salad bowl were chosen. As all fingers were involved the exploration process could be performed within less than a minute while acquiring still enough data points. During the exploration it was considered not to acquire too many data points as this significantly extends the amount of calculation time for the superquadric estimate. From the acquired data approximating superquadric representations were successfully estimated, as shown in figure 7.

The estimation algorithm could also handle incomplete surface point data as in case of the box, where it was not possible to acquire point data from the bottom side on which it was situated. The acquired data set comprised 176 points.

For the salad bowl the resulting data set comprised 472 points. As the superquadric function involved naturally only describes convex shapes the approximation of the salad bowl was rendered in the figure only in the representative range $\omega \; \epsilon \; [-\pi..0]$, which describes one half of the superellipsoid.

In case of the explored objects the extension coefficients a_1, a_2, a_3 of the superquadric model were in good correspondence to the dimensions of the real object.

It can be seen in the result plots, especially in figure 6 and 7, that the haptic point cloud exhibits basic noise and outliers

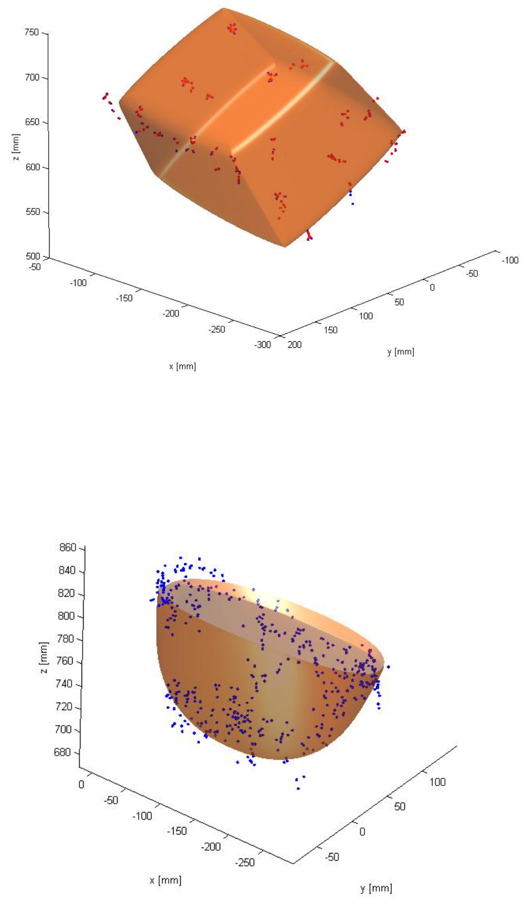

Fig. 7. Surface exploration data and superquadric approximation for a box and a salad bowl.

in some regions. From these experiments we found several reasons to affect the quality of the resulting point clouds:

1) The parametrization of our human hand model introduces a static error which could be minimized by adapting the model to the data glove's basic dimensions. Yet, hands of different individuals lead to irregular stretching of the glove fabric and occasionally to misalignment between finger joints and strain gauge sensors. This introduces a static model error which is not covered by the calibration process. We decided not to address this issue as our final goal is the operation of the system with a humanoid robot hand, where these problems cease to apply.
2) The measurement signals of the glove's strain gauge sensors are naturally afflicted with background noise which limits the resolution of physical features. We also expect this type of measurement noise for the joint angle sensors of our robot hand.
3) Beside the above, the pose data from visual tracking is superimposed by anisotropic interference as the estima-

tion of the wrists z-coordinate shows a significant higher amount of noise level than for the x- and y-coordinates, which is natural for stereo-camera systems. Also, some noise arises in the pose estimation, as the bracelet still has some clearance to move when worn by an individual. Further, estimation uncertainty increases if only a low number of markers can be detected in the scene, e.g. due to lighting conditions. The latter problems will become diminished when using a robot arm for exploration, as we can attach the marker band in a stable position and get additional pose information from joint angle sensors. This can be used in conjunction with the visual tracking system using data fusion.

IV. Conclusions and Future Work

In this paper we presented a framework for acquiring and estimating volumetric object models via haptic exploration by contour following. In a first evaluation results for haptic exploration of 2D and 3D shapes by a human subject wearing a data glove in an unstructured environment were described.

It could be shown that the underlying human hand model and the data acquisition process are sufficiently precise enough to acquire contact position data when exploring the shape of objects having the magnitude of dimension as the human hand does, while the exploration process could be performed using the modeled set of degrees of freedom of the human fingers. Further we could demonstrate fitting the acquired contact data to superquadric shapes.

As a next step we will address the transfer of the haptic exploration framework to our humanoid robot platform. The platform already incorporates the same stereo vision system as used for the experiments described in this paper. A tactile sensor system for the robot hand has been developed that provides more information over the binary switches deployed with exploration by a human.

Hence, the focus of our work will move to the development of autonomous and robust visually guided haptic exploration strategies for shape recovery by a humanoid robot with five-finger hands.

Acknowledgement

The work described in this paper was conducted within the EU Cognitive Systems project PACO-PLUS (FP6-2004-IST-4-027657) funded by the European Commission and the German Humanoid Research project (SFB 588) funded by the German Research Foundation (DFG: Deutsche Forschungsgemeinschaft).

References

[1] Susan J. Lederman and Roberta L. Klatzky, "Hand movements: A window into haptic object recognition," *Cognitive Psychology*, vol. 19, no. 3, pp. 342–368, 1987.

[2] P.K. Allen and K.S. Roberts, "Haptic object recognition using a multi-fingered dextrous hand," in *Robotics and Automation, 1989. Proceedings., 1989 IEEE International Conference on*, 14-19 May 1989, pp. 342–347 vol.1.

[3] S. Caselli, C. Magnanini, and F. Zanichelli, "Haptic object recognition with a dextrous hand based on volumetric shape representations," in *Multisensor Fusion and Integration for Intelligent Systems, 1994. IEEE International Conference on MFI '94.*, 2-5 Oct. 1994, pp. 280–287.

[4] David J. Montana, "The kinematics of contact and grasp," *International Journal of Robotics Research*, vol. 7, no. 3, pp. 17 – 32, June 1988.

[5] P.K. Allen, "Mapping haptic exploratory procedures to multiple shape representations," in *Robotics and Automation, 1990. Proceedings., 1990 IEEE International Conference on*, 13-18 May 1990, vol. 3, pp. 1679–1684.

[6] N. Chen, H. Zhang, and R. Rink, "Edge tracking using tactile servo," in *Intelligent Robots and Systems 95. 'Human Robot Interaction and Cooperative Robots', Proceedings. 1995 IEEE/RSJ International Conference on*, 5-9 Aug. 1995, vol. 2, pp. 84–89.

[7] A.M. Okamura and M.R. Cutkosky, "Haptic exploration of fine surface features," in *Robotics and Automation, 1999. Proceedings. 1999 IEEE International Conference on*, 10-15 May 1999, vol. 4, pp. 2930–2936.

[8] A. Petrovskaya, O. Khatib, S. Thrun, and A.Y. Ng, "Bayesian estimation for autonomous object manipulation based on tactile sensors," in *Robotics and Automation, 2006. ICRA 2006. Proceedings 2006 IEEE International Conference on*, May 15-19, 2006, pp. 707–714.

[9] T. Asfour, K. Regenstein, P. Azad, J. Schroder, A. Bierbaum, N. Vahrenkamp, and R. Dillmann, "Armar-iii: An integrated humanoid platform for sensory-motor control," in *Humanoid Robots, 2006 6th IEEE-RAS International Conference on*, Dec. 2006, pp. 169–175.

[10] Corey Goldfeder, Peter K. Allen, Claire Lackner, and Raphael Pelossof, "Grasp planning via decomposition trees," in *Robotics and Automation, 2007 IEEE International Conference on*, 10-14 April 2007, pp. 4679–4684.

[11] A. Kargov, T. Asfour, C. Pylatiuk, R. Oberle, H. Klosek, S. Schulz, K. Regenstein, G. Bretthauer, and R. Dillmann, "Development of an anthropomorphic hand for a mobile assistive robot," in *Rehabilitation Robotics, 2005. ICORR 2005. 9th International Conference on*, 28 June-1 July 2005, pp. 182–186.

[12]] J. Lee and T. Kunii, "Constraint-based hand animation," in *Models and Techniques in Computer Animation*, Tokyo, 1993, pp. 110–127, Springer, Tokyo.

[13] Y. Yasumuro, Qian Chen, and K. Chihara, "3d modeling of human hand with motion constraints," in *3-D Digital Imaging and Modeling, 1997. Proceedings., International Conference on Recent Advances in*, 12-15 May 1997, pp. 275–282.

[14] A. Erol, G. Bebis, M. Nicolescu, R.D. Boyle, and X. Twombly, "A review on vision-based full dof hand motion estimation," in *Computer Vision and Pattern Recognition, 2005 IEEE Computer Society Conference on*, 20-26 June 2005, vol. 3, pp. 75–75.

[15] M. Bray, E. Koller-Meier, and L. Van Gool, "Smart particle filtering for 3d hand tracking," in *Automatic Face and Gesture Recognition, 2004. Proceedings. Sixth IEEE International Conference on*, 17-19 May 2004, pp. 675–680.

[16] B. Buchholz and T.J. Armstrong, "A kinematic model of the human hand to evaluate its prehensile capabilities," *Journal of Biomechanics*, vol. 25, no. 2, pp. 149–162, 1992.

[17] J.J. Kuch and T.S. Huang, "Vision based hand modeling and tracking for virtual teleconferencing and telecollaboration," in *Computer Vision, 1995. Proceedings., Fifth International Conference on*, 20-23 June 1995, pp. 666–671.

[18] Michael Isard and Andrew Blake, "ICONDENSATION: Unifying low-level and high-level tracking in a stochastic framework," *Lecture Notes in Computer Science*, vol. 1406, pp. 893–908, 1998.

[19] A.H. Barr, "Superquadrics and angle-preserving transformations," *Computer Graphics and Applications, IEEE*, vol. 1, no. 1, pp. 11–23, Jan 1981.

[20] F. Solina and R. Bajcsy, "Recovery of parametric models from range images: the case for superquadrics with global deformations," *Pattern Analysis and Machine Intelligence, IEEE Transactions on*, vol. 12, no. 2, pp. 131–147, Feb. 1990.

[21] Donald W. Marquardt, "An algorithm for least-squares estimation of nonlinear parameters," *SIAM Journal on Applied Mathematics*, vol. 11, no. 2, pp. 431–441, 1963.

[22] A.D. Gross and T.E. Boult, "Error of fit measures for recovering parametric solids," in *Computer Vision., 1988. Second International Conference on*, December 5-8, 1988, pp. 690–694.